Astron. Astrophys. 329, 361–374 (1998)

ASTRONOMY
AND
ASTROPHYSICS

Galactic microlensing with rotating binaries

M. Dominik

Institut für Physik, Universität Dortmund, D-44221 Dortmund, Germany

Received 11 February 1997 / Accepted 5 August 1997

Abstract. The influence of rotating binary systems on the light curves of galactic microlensing events is studied. Three different rotating binary systems are discussed: a rotating binary lens, a rotating binary source, and the earth's motion around the sun (parallax effect). The most dramatic effects arise from the motion of a binary lens because of the changes of the caustic structure with time. I discuss when the treatment of a microlensing event with a static binary model is appropriate. It is shown that additional constraints on the unknown physical quantities of the lens system arise from a fit with a rotating binary lens as well as from the earth-around-sun motion. For the DUO#2 event, a fit with a rotating binary lens is presented.

Key words: gravitational lensing – dark matter – binaries: general – stars: low-mass, brown dwarfs – planetary systems

1. Introduction

It is a fact that mass objects in a binary system exhibit a rotation around their center of mass. However, this motion has mostly been neglected in discussions of binary sources and lenses in the context of galactic microlensing. Binary motion can play a role through a binary lens, a binary source, and the motion of the earth (with the observer on it) around the sun (parallax effect). Griest & Hu (1992) have presented an examplary light curve for a rotating binary source and have claimed that such events are rare. As we will see in this paper, however, the influence of the rotation effects increases with the event timescale. In addition, for the unknown halo population nothing is known about the distribution of parameters for hypothetical binary systems. Taking into account the large uncertainties in the position of the lens and the relative velocity between source, lens, and observer, the rotation effects cannot be neglected a-priori and fits with static models should be checked for consistency. In fact, an event showing the motion of the earth around the sun has already been detected (Alcock et. al. 1995) and the EROS#2 event can be explained by microlensing of an eclipsing binary (an even more special case of a rotating binary source) (Ansari et al. 1995). It is however doubtful, whether the EROS#2 event is due to microlensing at all (Paczyński 1996). In this paper I will discuss binary motion in the source, the lens, and in the earth-sun system (at the observer), where the most dramatic effects are caused by a rotating binary lens through the motion of the caustics.

In Sect. 2, a description of the binary motion is given, which is needed in the following sections. Sect. 3 reviews some basics of galactic microlensing. Sect. 4 shows the parametrization for rotating binary lens events and some examples for light curves. In Sect. 5, estimates are shown which help to decide whether the treatment of a binary lens as being static is appropriate. Sect. 6 discusses rotating binary sources in a similar way as for binary lenses. In Sect. 7, I also treat the earth-around-sun motion (parallax effect) which has been noted by Gould (1992) and observed by MACHO (Alcock et al. 1995). In Sect. 8, it is shown how additional information about physical parameters follows from the parameters for a rotating binary lens and from the parallax effect. For completeness, it is also noted that an additional constraint follows from the finite source size, if the physical size of the source is known. Sect. 9 finally presents a fit for the DUO#2 event using a rotating binary lens, which uses different parameters than the static binary fits already mentioned (Alard et. al 1995; Dominik 1997b). The appendix compares the parameters defined in Sect. 7 with the treatment of the parallax event by MACHO (Alcock et al. 1995).

2. Binary motion

In order to set the notation, I review some properties of the dynamics of binary systems (see eg. Landau & Lifshitz 1969, p. 29f.) in this section. Let us consider an object of mass μ_1 at $\boldsymbol{r}_1$ and an object of mass μ_2 at $\boldsymbol{r}_2$. The Lagrangian of this system is given by

$$L = \frac{1}{2}\mu_1 \dot{\boldsymbol{r}}_1{}^2 + \frac{1}{2}\mu_2 \dot{\boldsymbol{r}}_2{}^2 - V\left(|\boldsymbol{r}_1 - \boldsymbol{r}_2|\right) , \tag{1}$$

where V is the gravitational potential

$$V\left(|\boldsymbol{r}_1 - \boldsymbol{r}_2|\right) = -G\frac{\mu_1\mu_2}{|\boldsymbol{r}_1 - \boldsymbol{r}_2|} . \tag{2}$$

This is the Kepler problem.

Let $\boldsymbol{r}$ be the difference vector, $\boldsymbol{R}$ the coordinate of the center of mass, M the total mass and μ the reduced mass given by

$$\boldsymbol{r} = \boldsymbol{r}_1 - \boldsymbol{r}_2 \,, \tag{3}$$

$$\boldsymbol{R} = \frac{\mu_1 \boldsymbol{r}_1 + \mu_2 \boldsymbol{r}_2}{\mu_1 + \mu_2} \,, \tag{4}$$

$$M = \mu_1 + \mu_2 \,, \tag{5}$$

$$\mu = \frac{\mu_1 \mu_2}{\mu_1 + \mu_2} \,. \tag{6}$$

With these definitions, the Lagrangian can be written as

$$L = \frac{1}{2} M \dot{\boldsymbol{R}}^2 + \frac{1}{2} \mu \dot{\boldsymbol{r}}^2 - V(|\boldsymbol{r}|) \,. \tag{7}$$

The Euler-Lagrange equation for $\boldsymbol{R}$ is

$$0 = \frac{d}{dt} \frac{\partial L}{\partial \dot{R}_j} = \frac{d}{dt} \left(M \dot{R}_j \right) \,, \tag{8}$$

so that $\dot{\boldsymbol{R}} = \text{const.}$, i.e. the center of mass moves uniformly. If one chooses a coordinate system with the origin at the center of mass, one has $\boldsymbol{R} = 0$ and therefore

$$\boldsymbol{r}_1 = \frac{\mu_2}{\mu_1 + \mu_2} \boldsymbol{r} \quad \text{and} \quad \boldsymbol{r}_2 = -\frac{\mu_1}{\mu_1 + \mu_2} \boldsymbol{r} \,. \tag{9}$$

As can be seen from the Lagrangian, $\boldsymbol{r}(t)$ gives the motion of a particle of mass μ in the gravitational potential

$$V(|\boldsymbol{r}|) = -G \frac{\mu M}{|\boldsymbol{r}|} \,. \tag{10}$$

For a gravitationally bound system, the trajectory is an ellipse in a plane perpendicular to the angular momentum $\boldsymbol{L}$, where the origin (center of mass) is in a focus of the ellipse. Let ε be the eccentricity and a the semimajor axis. With polar coordinates (r, φ), the trajectory is given by

$$r(\varphi) = \frac{q}{1 + \varepsilon \cos \varphi} \,, \tag{11}$$

where $q = a(1 - \varepsilon^2)$. The minimal value is $r_{\min} = a(1 - \varepsilon)$ obtained for $\varphi = 0$, and the maximal value is $r_{\max} = a(1 + \varepsilon)$ obtained for $\varphi = \pi$.

Therefore, one can parametrize the curve with a parameter ξ as

$$r(\xi) = a(1 - \varepsilon \cos \xi) \,. \tag{12}$$

The components along the semimajor axis (x-direction) and the semiminor axis (y-direction) follow as

$$x(\xi) = a(\cos \xi - \varepsilon) \,, \tag{13}$$

$$y(\xi) = a \sqrt{1 - \varepsilon^2} \sin \xi \,. \tag{14}$$

The time dependence is given by

$$t = \sqrt{\frac{a^3}{GM}} \, (\xi - \varepsilon \sin \xi) \,, \tag{15}$$

so that $t = 0$ corresponds to the point $(r_{\min}, 0)$. One sees that in general this equation cannot be solved analytically for ξ to yield $x(t)$ and $y(t)$ but instead has to be solved numerically. Changing ξ to $\xi + 2\pi$ corresponds to one revolution, so that the period is given by

$$T = 2\pi \sqrt{\frac{a^3}{GM}} \,. \tag{16}$$

Since, for $n \in \mathbb{Z}$, $x(\xi + n2\pi) = x(\xi)$ and $y(\xi + n2\pi) = y(\xi)$ one can subtract full periods n from the given time t and solve

$$t' = t - nT = \sqrt{\frac{a^3}{GM}} \, (\xi - \varepsilon \sin \xi) \tag{17}$$

for a $\xi \in [0, 2\pi)$. With

$$\lfloor x \rfloor = k \quad \text{with} \quad k \in \mathbb{Z}, k \le x < k + 1 \tag{18}$$

and the period T, Eq. (17) can be written as

$$2\pi \left(\frac{t}{T} - \left\lfloor \frac{t}{T} \right\rfloor \right) = \xi - \varepsilon \sin \xi \,. \tag{19}$$

For $\xi = 0$ at $t = t_0$ one has

$$2\pi \left(\frac{t - t_0}{T} - \left\lfloor \frac{t - t_0}{T} \right\rfloor \right) = \xi - \varepsilon \sin \xi \,. \tag{20}$$

For $\xi = \xi_0$ at $t = t_1$, $\xi = 0$ is obtained for

$$t_0 = t_1 - \frac{T}{2\pi} (\xi_0 - \varepsilon \sin \xi_0) \,, \tag{21}$$

so that

$$2\pi \left(\frac{t - t_1}{T} - \left\lfloor \frac{t - t_1}{T} + \frac{1}{2\pi} (\xi_0 - \varepsilon \sin \xi_0) \right\rfloor \right) + \\ + \xi_0 - \varepsilon \sin \xi_0 = \xi - \varepsilon \sin \xi \tag{22}$$

will yield a $\xi \in [0, 2\pi)$.

Let $r = |\boldsymbol{r}|$ and $v = |\dot{\boldsymbol{r}}|$. The total energy E, which is the sum of the kinetic energy T and the potential energy V

$$E = T + V = \frac{1}{2} \mu v^2 - \frac{G \mu M}{r} \,, \tag{23}$$

is related to the semimajor axis a by

$$E = -\frac{G \mu M}{2a} \,. \tag{24}$$

From Eq. (23) and Eq. (24), and with

$$v_{\text{circ}} = \frac{2\pi}{T} \, a \,, \tag{25}$$

the velocity as a function of r reads

$$v(r) = v_{\text{circ}} \sqrt{\frac{2a}{r} - 1} \,. \tag{26}$$

Table 1. The ratio ρ_v between the maximal and the minimal velocity for different eccentricities ε

ε	ρ_v
0	1.000
0.01	1.020
0.05	1.105
0.1	1.111
0.2	1.500
0.3	1.857
0.4	2.333
0.5	3.000
0.6	4.000
0.7	5.667
0.8	9.000
0.9	19.000

The maximal velocity is obtained for $r_{\rm min}$ as

$$v_{\rm max} = v(r_{\rm min}) = v_{\rm circ}\,\sqrt{\frac{1+\varepsilon}{1-\varepsilon}}\,, \tag{27}$$

and the minimal velocity is obtained for $r_{\rm max}$ as

$$v_{\rm min} = v(r_{\rm max}) = v_{\rm circ}\,\sqrt{\frac{1-\varepsilon}{1+\varepsilon}}\,, \tag{28}$$

The ratio between $v_{\rm max}$ and $v_{\rm min}$ is

$$\rho_v = \frac{v_{\rm max}}{v_{\rm min}} = \frac{1+\varepsilon}{1-\varepsilon}\,. \tag{29}$$

Values for ρ_v for different eccentricities ε are shown in Table 1. From the virial theorem, one obtains for the expectation values of the kinetic and the potential energy the relation

$$2\ <T> = -\,<V>\,, \tag{30}$$

so that one obtains for the radius r and the velocity v the relations

$$<\frac{1}{r}> = \frac{1}{a}\,, \tag{31}$$

and

$$<v^2> = \frac{GM}{a} = \frac{4\pi^2}{T^2}\,a^2 = v_{\rm circ}^2\,. \tag{32}$$

3. Some basics of gravitational lensing

The effect of light bending by a point mass M at the distance $D_{\rm d}$ from the observer and at distance $D_{\rm ds}$ from the source object which is located at a distance $D_{\rm s}$ from the observer can be described by the gravitational lens equation

$$\boldsymbol{y} = \boldsymbol{x} - \frac{\boldsymbol{x}}{|\boldsymbol{x}|^2}\,, \tag{33}$$

(e.g. Schneider et al. 1992), where $\boldsymbol{y}$ is a dimensionless coordinate in the plane perpendicular to the line-of-sight observer-lens at the position of the source (source plane) and $\boldsymbol{x}$ is a dimensionless coordinate in a corresponding plane at the position of the lens (lens plane). The physical position of the light ray connecting the source and the observer is given by

$$\boldsymbol{\xi} = r_{\rm E}\,\boldsymbol{x} \tag{34}$$

in the lens plane and

$$\boldsymbol{\eta} = \frac{D_{\rm s}}{D_{\rm d}}\,r_{\rm E}\,\boldsymbol{y} = r'_{\rm E}\,\boldsymbol{y}\,. \tag{35}$$

In these equations, $r_{\rm E}$ denotes the Einstein radius, given by

$$r_{\rm E} = \sqrt{\frac{4GM}{c^2}\,\frac{D_{\rm d}\,D_{\rm ds}}{D_{\rm s}}}\,, \tag{36}$$

and $r'_{\rm E} = \frac{D_{\rm s}}{D_{\rm d}}\,r_{\rm E}$ denotes the projected Einstein radius. For a system of N lenses at positions $\boldsymbol{x}^{(i)}$ with mass fractions m_i, the lens equation reads

$$\boldsymbol{y} = \boldsymbol{x} - \sum_{i=1}^{N} \frac{\boldsymbol{x}-\boldsymbol{x}^{(i)}}{|\boldsymbol{x}-\boldsymbol{x}^{(i)}|^2}\,. \tag{37}$$

Let $v_\perp$ be the velocity of the relative motion between lens, source, and observer as measured in the lens plane. If one considers a coordinate system in which the observer and the source are at rest, $v_\perp$ gives the relative motion of the lens. Alternatively, one can consider a coordinate system in which the observer and the lens are at rest, so that $v_\perp$ gives the motion of the source position as projected onto the lens plane. In either case, a characteristic timescale of the motion (and therefore of the event) is given by

$$t_{\rm E} = \frac{r_{\rm E}}{v_\perp}\,. \tag{38}$$

This definition means that the moving object transverses one Einstein radius in the lens plane in the time $t_{\rm E}$.

Let $t_{\rm max}$ denote the time at the closest approach to the line-of-sight and $u_{\rm min}$ the impact parameter at $t_{\rm max}$ in units of the Einstein radius $r_{\rm E}$. For a point source and a point-mass lens, one obtains for the impact parameter at time t

$$u(t) = \sqrt{u_{\rm min}^2 + [p(t)]^2} \tag{39}$$

with

$$p(t) = \frac{t - t_{\rm max}}{t_{\rm E}}\,, \tag{40}$$

and the amplification is given by (e.g. Paczyński 1986)

$$A(u) = \frac{u^2+2}{u\sqrt{u^2+4}}\,. \tag{41}$$

The light curve for an event involving a point source and a point-mass lens is therefore described by the 3 parameters $t_{\rm E}$, $t_{\rm max}$, and $u_{\rm min}$.

4. Rotating binary lenses

For a rotating binary lens, one needs the projection of the trajectory onto the lens plane. The orientation of the rotating system relative to the lens plane is given by two angles β and γ. For $\beta = 0$ and $\gamma = 0$, x is chosen along x_1, y along x_2 and the angular momentum $\boldsymbol{L}$ is towards the observer (x_3-direction). The angle β describes a rotation of the lens system around x_1 and the angle γ a following rotation of the lens system around x_2. This means that one has the transformation

$$\begin{pmatrix} x_1 \\ x_2 \\ x_3 \end{pmatrix} = \frac{1}{r_\mathrm{E}} \mathscr{R}_1 \begin{pmatrix} x \\ y \\ z \end{pmatrix} \tag{42}$$

with

$$\mathscr{R}_1 = \begin{pmatrix} \cos\gamma & \sin\beta\sin\gamma & \cos\beta\sin\gamma \\ 0 & \cos\beta & -\sin\beta \\ -\sin\gamma & \sin\beta\cos\gamma & \cos\beta\cos\gamma \end{pmatrix} . \tag{43}$$

Since $z = 0$ and the x_3-value is redundant, the transformation reduces to

$$\begin{pmatrix} x_1 \\ x_2 \end{pmatrix} = \frac{1}{r_\mathrm{E}} \begin{pmatrix} \cos\gamma & \sin\beta\sin\gamma \\ 0 & \cos\beta \end{pmatrix} \begin{pmatrix} x \\ y \end{pmatrix} . \tag{44}$$

A rotation around x_3 is not considered here, since it can be put into the orientation α of the source trajectory.

Altogether, one needs the following parameters for lensing by a rotating binary lens:

- The point of time t_b of the closest approach of the source to the center of mass of the lens system,
- the characteristic time $t_\mathrm{E} = r_\mathrm{E}/v_\perp$,
- the mimimal projected distance b in the lens plane between source and center of mass of the lens system in units of the Einstein radius,
- the angle α between the x_1-direction and the direction of the projected source trajectory,
- the mass fraction $m_1 = \mu_1/M$,
- the semimajor axis in units of the Einstein radius $\rho = a/r_\mathrm{E}$,
- the rotation angle β,
- the rotation angle γ,
- the period T,
- the eccentricity ε,
- the phase ξ_0 at $t = t_b$.

Compared with the static binary lens, one needs 5 additional parameters.

The position of a hypothetical object of mass μ is therefore, using Eqs. (13), (14), and (44),

$$x_1(t) = \rho\Big[\cos\gamma(\cos\xi(t) - \varepsilon) + \\ + \sin\beta\sin\gamma\sqrt{1-\varepsilon^2}\sin\xi(t)\Big] , \tag{45}$$

$$x_2(t) = \rho\cos\beta\sqrt{1-\varepsilon^2}\sin\xi(t) , \tag{46}$$

and, with Eq. (9), the positions of the masses μ_1 and μ_2 are

$$\boldsymbol{x}^{(1)}(t) = (1-m_1)\boldsymbol{x}(t) , \quad \boldsymbol{x}^{(2)}(t) = -m_1\boldsymbol{x}(t) . \tag{47}$$

From Eq. (22), the value of $\xi \in [0, 2\pi)$ for a given t is given by

$$2\pi\left(\frac{t-t_b}{T} - \left\lfloor \frac{t-t_b}{T} + \frac{1}{2\pi}(\xi_0 - \varepsilon\sin\xi_0)\right\rfloor\right) + \\ + \xi_0 - \varepsilon\sin\xi_0 = \xi - \varepsilon\sin\xi . \tag{48}$$

Examples for rotating binary lenses are shown in Figs. 1 and 2. For both figures, $\beta = \gamma = \varepsilon = \xi_0 = 0$, and ρ has been chosen as 2χ. For Fig. 1, the lens model BL for the MACHO LMC#1 event has been used (Dominik & Hirshfeld 1996), so that $t_\mathrm{E} = 16.27\ d$, $t_b = 433.18$, $\rho = 0.4077$, $m_1 = 0.463$, $\alpha = 1.151$, $b = 0.146$, and $m_\mathrm{base} = 4.5170$. m_base denotes the negative observed magnitude at the unlensed state and f the contribution of the source to the total light at unlensed state. The rotation period has been chosen as $T = 365$ d, 100 d, 50 d, and 25 d. For Fig. 2, the lens model BL0 for the OGLE#7 event has been used (Dominik 1997b)[1], so that $t_\mathrm{E} = 80.88\ d$, $t_b = 1173.25$, $\rho = 1.131$, $m_1 = 0.506$, $\alpha = 2.297$, $b = 0.048$, $f = 0.557$, and $m_\mathrm{base} = -17.5171$. The rotation period has been chosen as $T = 3000$ d, 1000 d, 365 d, and 100 d.

One sees that dramatic effects occur if the period is small, especially if additional caustic crossings occur. But even for a period of 365 days, a deviation from the MACHO LMC#1-fit is visible, and for a period of 1000 days a second peak for parameters near the OGLE#7-fit occurs. This constellation looks a little like the DUO#2 event. A corresponding model is discussed in Sect. 9. Note that the rotation period is about 12 times larger than the timescale t_E for this constellation, nevertheless a dramatic effect occurs in the light curve. Note also that the example used by Griest & Hu (1992) for rotating binary sources used a period T which is 4 times smaller than t_E.

5. When is the rotation effect negligible?

Let us consider a fit for a static binary lens. As discussed by Dominik (1997a), cited as D97a in the following, the rotation period T can be estimated using the timescale t_E and distributions of the lens position and the velocity $v_\perp$. In a similar way, one can also obtain probability distributions for the ratio of the timescales

$$R_T = \frac{t_\mathrm{E}}{T} , \tag{49}$$

and the ratio of the velocities of the binary motion of the lens and the perpendicular motion with respect to the line-of-sight

$$R_v = \frac{v_\mathrm{circ}}{v_\perp} . \tag{50}$$

Note that irrespective of the eccentricity $<v^2>= v_\mathrm{circ}^2$, and the maximal and minimal velocities are of the same order for moderate eccentricities as shown in Sect. 2. The projection of the velocity of the lens system to a plane perpendicular to the line-of-sight may be lower than this, but the velocity is perpendicular to the line-of-sight at least twice a period. Expressing R_T and

[1] This model coincides with that of Alard et. al (1995).

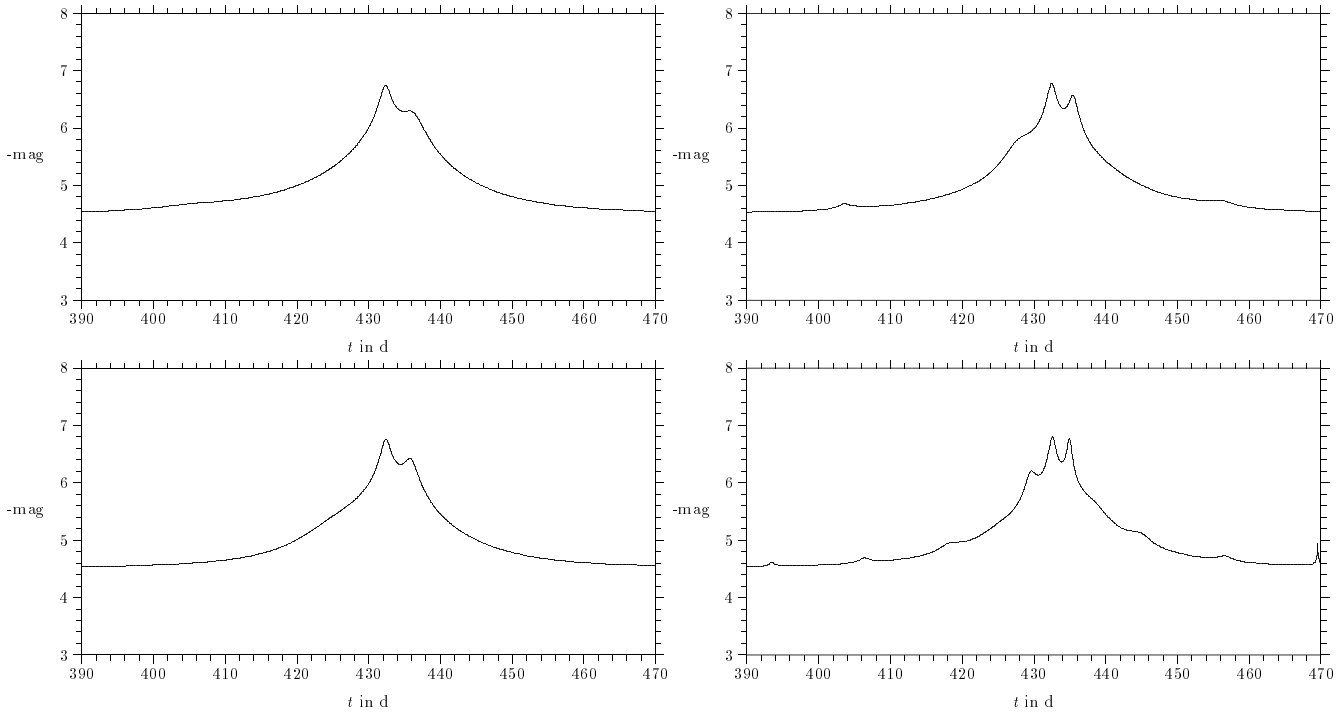

Fig. 1a–d. Rotating binary lenses with parameters as for the BL-fit of MACHO LMC#1. $\beta = \gamma = \varepsilon = \xi_0 = 0$. **a** $T = 365$ d, **b** $T = 100$ d, **c** $T = 50$ d, **d** $T = 25$ d.

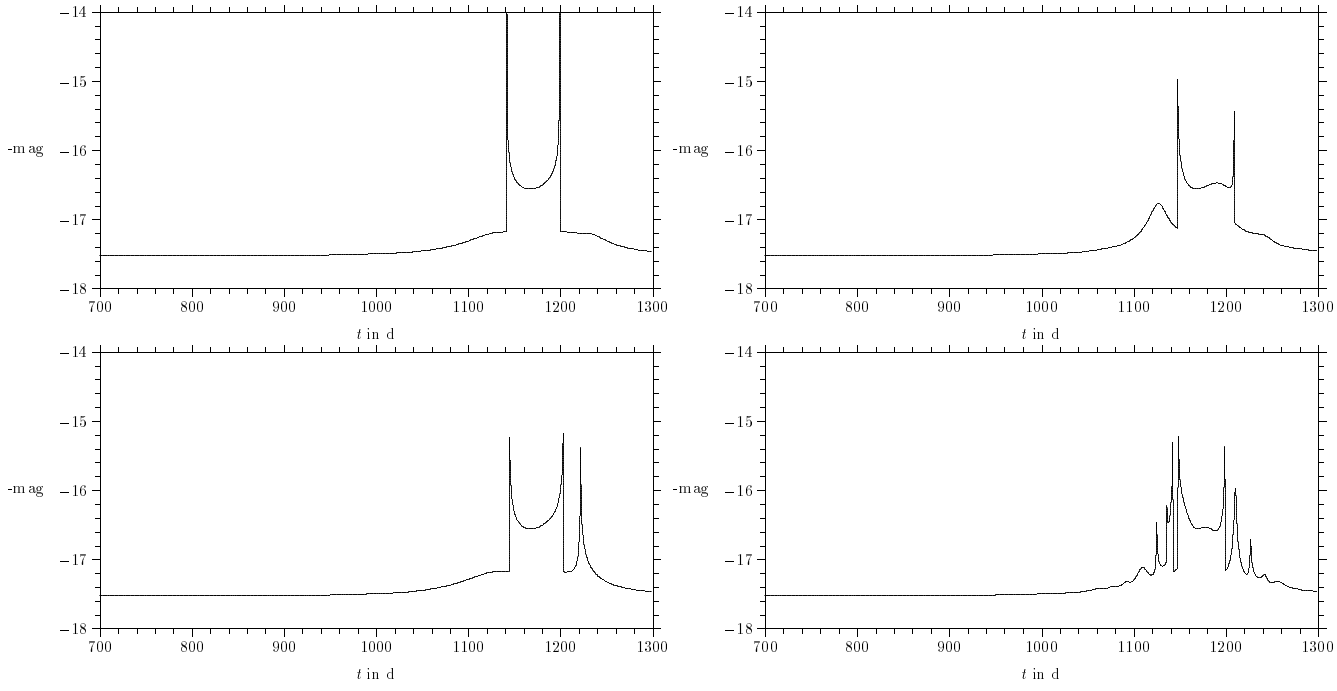

Fig. 2a–d. Rotating binary lenses with parameters as for the BL0-fit of OGLE#7. $\beta = \gamma = \varepsilon = \xi_0 = 0$. **a** $T = 3000$ d, **b** $T = 1000$ d, **c** $T = 365$ d, **d** $T = 100$ d.

R_v in terms of the fit parameters, the lens distance $x = D_\mathrm{d}/D_\mathrm{s}$, and the dimensionless velocity parameter $\zeta = v_\perp/v_\mathrm{c}$ (where v_c is a characteristic velocity), yields

$$R_T = \frac{c}{4\pi}\sqrt{\frac{t_\mathrm{E}}{\rho^3\, D_\mathrm{s}\, v_\mathrm{c}\, x(1-x)\,\zeta}}\,, \tag{51}$$

and

$$R_v = \frac{c}{2}\sqrt{\frac{t_\mathrm{E}}{\rho\, D_\mathrm{s}\, v_\mathrm{c}\, x(1-x)\,\zeta}}\,. \tag{52}$$

One sees that

$$R_v = 2\pi\rho\, R_T\,. \tag{53}$$

Note that there are two problems with these quantities. First, as discussed above, the projected trajectory of the binary components are not circles. Second, from fits with static binary models, one only gets the projected distance 2χ between the objects, where $\rho \geq \chi$ in general and $\rho = 2\chi$ for circular projected trajectories.

Since $R_T, R_v \propto \sqrt{t_\mathrm{E}}$ and $R_T \propto \sqrt{1/\rho^3}$, $R_v \propto \sqrt{1/\rho}$, the rotation of binary lenses is most important for events with long t_E and small ρ.[2]

Since R_T and R_v are of the form

$$G(t_\mathrm{E}, x, \zeta) = G_0(t_\mathrm{E})\,[x(1-x)]^k\,\zeta^l \tag{54}$$

with $k = l = -\frac{1}{2}$, estimates and probability distributions can be derived using the approach presented in D97a. Let $H(x)\,dx$ be the probability for finding x in $[x, x+dx]$ (where $H(x)$ is proportional to the mass density $\rho(x)$)[3], $\widetilde{K}(\zeta)\,d\zeta$ be the probability for finding ζ in $[\zeta, \zeta+d\zeta]$, and let $T(r,s)$ be defined as

$$T(r,s) = \int [x(1-x)]^r\; H(x)\,\zeta^s\,\widetilde{K}(\zeta)\,d\zeta\,dx\,, \tag{55}$$

which separates as

$$T(r,s) = \Xi(r)\,W(s)\,, \tag{56}$$

where

$$\Xi(r) \;=\; \int [x(1-x)]^r\; H(x)\,dx\,, \tag{57}$$

$$W(s) \;=\; \int \zeta^s\,\widetilde{K}(\zeta)\,d\zeta\,, \tag{58}$$

if the velocity distribution does not depend on x. Following D97a, the expectation values for a quantity G assuming an unknown mass distribution are given by

$$<G> = G_0\,\frac{T(k+1,l)}{\Xi(1)} = G_0\,F(-1,k,l)\,. \tag{59}$$

[2] It is implied that one has an effect from binarity. For $\rho \to 0$, this effect vanishes. However, if one sees the binarity, the rotation is especially important for small ρ.

[3] $H(x) = \rho(x)/\rho_0$, where ρ_0 is an arbitrary characteristic mass density, so that at the distance x_0, where $\rho(x_0) = \rho_0$, one has $H(x_0) = 1$.

Let us adopt the simple galactic halo model of D97a with a velocity distribution of

$$\widetilde{K}(\zeta) = 2\zeta\,\exp\left\{-\zeta^2\right\} \tag{60}$$

where v_c has been chosen so that $<v_\perp^2> = v_\mathrm{c}^2$, and the mass density of halo objects being

$$\rho(r) = \rho_0\,\frac{R_\mathrm{GC}^2}{r^2}\,, \tag{61}$$

where r measures the distance from the Galactic center, R_GC is the distance from the sun to the Galactic center, and ρ_0 is the local density at the position of the sun. With the values $D_\mathrm{s} = 50$ kpc and $R_\mathrm{GC} = 10$ kpc, and the halo being extended up to the LMC, located at 82° from the Galactic center as seen from the observer, one obtains $\Xi(\frac{1}{2}) = 0.105$, $\Xi(1) = 0.0407$, $W(-\frac{1}{2}) = 1.225$ and therefore $F(-1,-\frac{1}{2},-\frac{1}{2}) = 3.16$. Using slightly different values for D_s (55 kpc) and R_GC (8.5 kpc), and varying the core radius a between 0 and 8 kpc yields estimates which differ by about 5 %.

For the expectation values, one obtains

$$<R_T> \;=\; 1.23\cdot 10^{-3}\,\rho^{-3/2}\,\left(\frac{v_\mathrm{c}}{210\ \mathrm{km/s}}\right)^{-1/2}\,\left(\frac{t_\mathrm{E}}{1\ \mathrm{d}}\right)^{1/2} \tag{62}$$

$$<R_v> \;=\; 7.74\cdot 10^{-3}\,\rho^{-1/2}\,\left(\frac{v_\mathrm{c}}{210\ \mathrm{km/s}}\right)^{-1/2}\,\left(\frac{t_\mathrm{E}}{1\ \mathrm{d}}\right)^{1/2} \tag{63}$$

The probability density for

$$\kappa_R = R_T/<R_T> = R_v/<R_v> \tag{64}$$

is given in D97a as

$$p(\kappa_R) = \frac{4\,[\Xi(1)]^3}{\left[\Xi(\frac{1}{2})\,W(-\frac{1}{2})\right]^4}\,\kappa_R^{-5}\int \frac{H(x)}{x(1-x)}\;\cdot$$
$$\cdot\,\exp\left\{-\left(\frac{1}{\kappa_R\sqrt{x(1-x)}}\,\frac{\Xi(1)}{\Xi(\frac{1}{2})\,W(-\frac{1}{2})}\right)^4\right\}dx\,, \tag{65}$$

and the probability density for $\lambda_R = \lg\kappa_R$ is given as

$$\psi(\lambda_R) = \frac{4\,\ln 10}{10^{4\lambda_R}}\,\frac{[\Xi(1)]^3}{\left[\Xi(\frac{1}{2})\,W(-\frac{1}{2})\right]^4}\int \frac{H(x)}{x(1-x)}\;\cdot$$
$$\cdot\,\exp\left\{-\left(\frac{1}{10^{\lambda_R}\sqrt{x(1-x)}}\,\frac{\Xi(1)}{\Xi(\frac{1}{2})\,W(-\frac{1}{2})}\right)^4\right\}dx\,. \tag{66}$$

These probability densities are shown in Fig. 3, where symmetric intervals around $<R_T>$ or $<R_v>$ containing probabilities of 68.3 % and 95.4 % respectively are shown for λ_R. The bounds of these intervals are also shown in Table 2. The smallest and the largest value in the 95.4 %-interval differ by a factor of about 5.

For the binary lens fits to MACHO LMC#1 (Dominik & Hirshfeld 1996), one obtains the values shown in Table 3. Since the true semimajor axis $a = \rho\, r_\mathrm{E}$ is not yielded by the fit, the

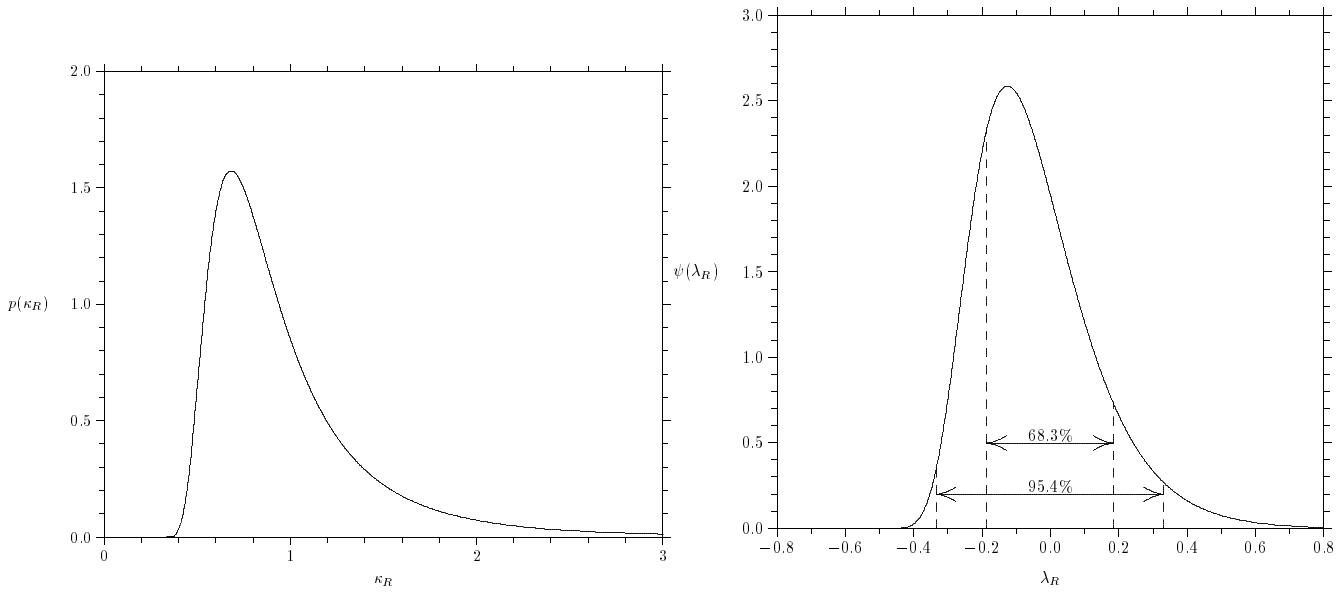

Fig. 3a and b. The probability densities **a** $p(\kappa_R)$ (left) and **b** $\psi(\lambda_R)$ (right) with symmetric 68.3 % and 95.4 % intervals around $<R_T>$ or $<R_v>$

Table 2. The bounds of symmetric intervals around $<R_T>$ or $<R_v>$ on a logarithmic scale which correspond to probabilities of 68.3 % and 95.4 %

$\Delta\lambda_{68.3}$	$\Delta\lambda_{95.4}$	$10^{-\Delta\lambda_{68.3}}$	$10^{\Delta\lambda_{68.3}}$	$10^{-\Delta\lambda_{95.4}}$	$10^{\Delta\lambda_{95.4}}$
0.1844	0.3317	0.654	1.53	0.466	2.15

Table 3. MACHO LMC#1: Estimates of R_T and R_v for different binary lens models.

	BL	BL1	BA	BA1	BA2
$t_{\rm E}$ [d]	16.27	17.53	685	155	35.7
$t_{\rm E}^{(2)}$ [d]	—	—	17.57	15.15	17.72
$<R_T>$	0.054	0.050	0.0086	0.0047	0.0030
$<R_v>$	0.069	0.069	0.13	0.065	0.034

estimates refer to $\rho = \chi$, which corresponds to a minimal value of the period $T_{\rm min}$, because $\rho \geq \chi$ for any gravitationally bound system and $T \propto \rho^{3/2}$. The timescale $t_{\rm E}^{(2)}$ corresponds to the Einstein radius of the smaller mass with mass fraction $1 - m_1$,

$$t_{\rm E}^{(2)} = t_{\rm E}\,\sqrt{1-m_1}\,. \tag{67}$$

One sees that the rotation is not likely to play a dominant effect, however a marginal effect may show up. For the wide binary models (BA, BA1, BA2), the peak arises from the passage near the smaller mass on a timescale $t_{\rm E}^{(2)}$, so that the influence from the binary rotation on the peak will be smaller than estimated using $t_{\rm E}$.

6. Rotating binary sources

In their discussion of binary sources, Griest & Hu (1992) have also mentioned their rotation. Here I show that the parameters for a rotating binary source can be chosen in analogy to the rotating binary lens. Let the relative motion of the lens perpendicular to the source-observer-line projected to the source plane be

$$\boldsymbol{y}^{\,(\rm lens)}(t) = \begin{pmatrix}\cos\widetilde{\alpha}\\ \sin\widetilde{\alpha}\end{pmatrix}\,\frac{t-\widetilde{t_b}}{t_{\rm E}} \;+\; \begin{pmatrix}-\sin\widetilde{\alpha}\\ \cos\widetilde{\alpha}\end{pmatrix}\,\widetilde{b}\,, \tag{68}$$

where $\widetilde{t_b}$ is the point of time of closest approach to the center of mass of the binary source system. The orientation of the rotating system relative to the source plane is given by two angles $\widetilde{\beta}$ and $\widetilde{\gamma}$. For $\widetilde{\beta} = 0$ and $\widetilde{\gamma} = 0$, x is chosen along y_1, y along y_2 and the angular momentum $\boldsymbol{L}$ is towards the observer (y_3-direction). The angle $\widetilde{\beta}$ describes a rotation of the source system around y_1 and the angle $\widetilde{\gamma}$ a following rotation of the source system around y_2. As for the rotating binary lens, one has the transformation

$$\begin{pmatrix}y_1\\ y_2\end{pmatrix} = \frac{1}{r'_{\rm E}}\,\begin{pmatrix}\cos\widetilde{\gamma} & \sin\widetilde{\beta}\sin\widetilde{\gamma}\\ 0 & \cos\widetilde{\beta}\end{pmatrix}\begin{pmatrix}x\\ y\end{pmatrix}\,. \tag{69}$$

A rotation around y_3 need not to be considered here, since it can be put into the orientation $\widetilde{\alpha}$ of the lens trajectory.

For lensing of a rotating binary source one needs the following parameters:

- The point of time $\widetilde{t_b}$ of the closest approach of the lens to the center of mass of the source system,
- the characteristic time $t_{\rm E} = r_{\rm E}/v_\perp$,
- the mimimal projected distance $\widetilde{b}$ in the source plane between lens and center of mass of the source system in units of the projected Einstein radius,

– the angle $\widetilde{\alpha}$ between the y_1-direction and the direction of the projected lens trajectory,
– the luminosity offset ratio ω,
– the mass fraction $\widetilde{m}_1$ of source object 1,
– the semimajor axis in units of the projected Einstein radius $\widetilde{\rho} = a/r'_{\rm E}$,
– the rotation angle $\widetilde{\beta}$,
– the rotation angle $\widetilde{\gamma}$,
– the period $\widetilde{T}$,
– the eccentricity $\widetilde{\varepsilon}$,
– the phase $\widetilde{\xi}_0$ at $t = \widetilde{t}_b$.

Compared with the static binary source, one needs 6 additional parameters.

From Eqs. (13), (14), and (69), the position of a hypothetical object of the reduced mass is given by

$$y_1(t) = \widetilde{\rho}\Big[\cos\widetilde{\gamma}(\cos\xi(t) - \widetilde{\varepsilon}) + \\ + \sin\widetilde{\beta}\sin\widetilde{\gamma}\sqrt{1-\widetilde{\varepsilon}^2}\sin\xi(t)\Big]\,, \quad (70)$$

$$y_2(t) = \widetilde{\rho}\cos\widetilde{\beta}\sqrt{1-\widetilde{\varepsilon}^2}\sin\xi(t)\,, \quad (71)$$

and the positions of the source objects 1 and 2 are, using Eq. (9),

$$\boldsymbol{y}^{(1)}(t) = (1-\widetilde{m}_1)\,\boldsymbol{y}(t)\,, \quad \boldsymbol{y}^{(2)}(t) = -\widetilde{m}_1\,\boldsymbol{y}(t)\,. \quad (72)$$

Note that for $\widetilde{\xi}_0 = 0$ and $\widetilde{\beta} = \widetilde{\gamma} = 0$, one obtains $y_1(\widetilde{t}_b) = \widetilde{\rho}(1-\widetilde{\varepsilon})$ and $y_2(\widetilde{t}_b) = 0$, so that object 2 is found left from object 1 on the y_1-axis, as for the binary lens. The value of $\xi \in [0, 2\pi)$ for a given t is obtained from (see Eq. (22))

$$2\pi\left(\frac{t-\widetilde{t}_b}{\widetilde{T}} - \left\lfloor\frac{t-\widetilde{t}_b}{\widetilde{T}} + \frac{1}{2\pi}\left(\widetilde{\xi}_0 - \widetilde{\varepsilon}\sin\widetilde{\xi}_0\right)\right\rfloor\right) + \\ + \widetilde{\xi}_0 - \widetilde{\varepsilon}\sin\widetilde{\xi}_0 = \xi - \widetilde{\varepsilon}\sin\xi\,. \quad (73)$$

The distance of the source objects from the projected lens position is given by

$$u_1(t) = \left|\boldsymbol{y}^{(\rm lens)}(t) - \boldsymbol{y}^{(1)}(t)\right| \quad (74)$$

and

$$u_2(t) = \left|\boldsymbol{y}^{(\rm lens)}(t) - \boldsymbol{y}^{(2)}(t)\right|\,. \quad (75)$$

For a point-mass lens these values can be directly inserted into the expression for the magnification A of a point-mass lens (see e.g. Paczyński 1986; Griest & Hu 1992)

$$A(u) = \frac{u^2+2}{u\sqrt{u^2+4}}\,. \quad (76)$$

Due to the absence of extended caustics, the effect of a rotating binary source and a point-mass lens is less dramatic than for a rotating binary lens. Examples are shown in Fig. 4. The parameters have been chosen, so that one gets a binary source fit for OGLE#5 for $\widetilde{T} \to \infty$ as trans-configuration [4]. This means

[4] The cis-trans-symmetry for binary sources has been discussed by Dominik & Hirshfeld (1996).

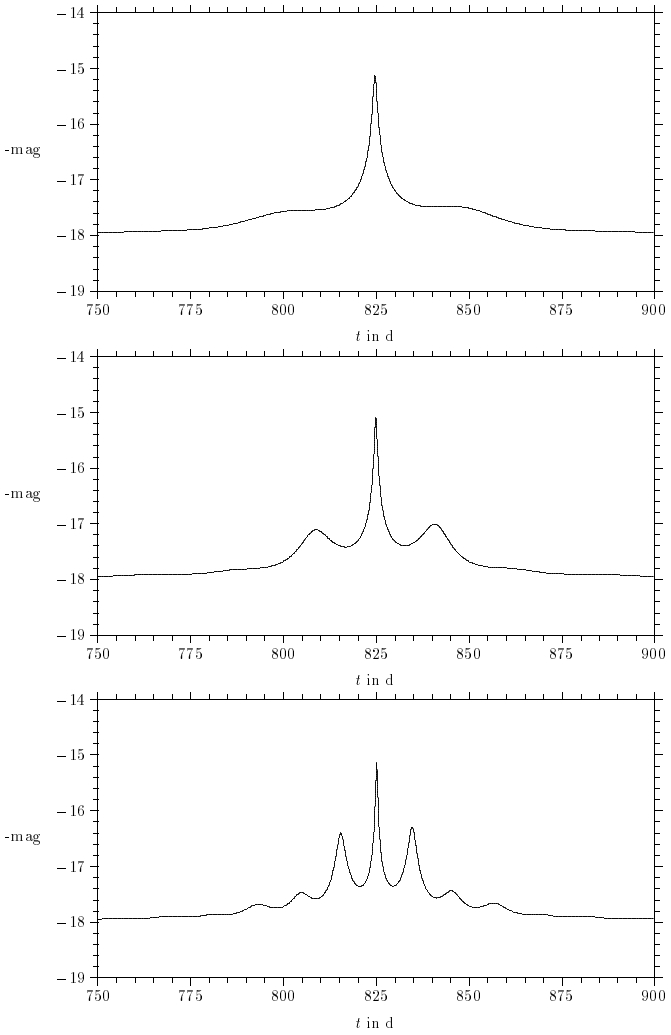

Fig. 4a–c. Rotating binary sources with parameters as for a binary source fit for OGLE#5 (trans-configuration). $\widetilde{\beta} = \widetilde{\gamma} = \widetilde{\varepsilon} = \widetilde{\xi}_0 = 0$, and $\widetilde{m}_1 = 0.5$. **a** $T = 100$ d, **b** $T = 50$ d, **c** $T = 25$ d.

that $t_{\rm E} = 26.27$, $\widetilde{\alpha} = 1.4512$, $\widetilde{t}_b = 825.719$ d, $\widetilde{b} = 0.4624$, $\omega = 0.3819$, and $m_{\rm base} = -17.9576$. $\widetilde{\rho} = 0.8679$ has been chosen so that $\widetilde{\rho}$ is the distance in the static case and $\widetilde{m}_1 = 0.5$. $\widetilde{\beta}$, $\widetilde{\gamma}$, $\widetilde{\varepsilon}$, and $\widetilde{\xi}_0$ have been chosen as zero and $\widetilde{T}$ takes the values 100 d, 50 d and 25 d.

7. The parallax effect

7.1. Parameters

The annual motion of the observer (on the earth) around the sun gives another effect of rotating binaries. It has been mentioned by Gould (1992) and observed by the MACHO collaboration (Alcock et al. 1995). In contrast to the other cases of a rotating lens or a rotating source, one knows most of the parameters of the binary system:

– the rotation period T,
– the semimajor axis $a_\oplus$,

– the eccentricity ε,
– the point of time when the earth is in perihelion t_p.

One also knows the position of the source of light characterized by

– the longitude φ measured in the ecliptic plane from the perihelion towards the earth's motion,
– the latitude χ measured from the ecliptic plane towards the ecliptic north.

A fit to an observed light curve for a parallax event involves two additional fit parameters:

– the length of the semimajor axis projected to the lens plane measured in Einstein radii ρ',
– a rotation angle ψ in the lens plane describing the relative orientation of $\boldsymbol{v}_\perp$ to the sun-earth system.

A displacement of the observer's position by $\boldsymbol{\delta}_\mathrm{O}$ is equivalent to a displacement of the source position projected to the lens plane by

$$\boldsymbol{\delta}_\mathrm{L} = \frac{D_\mathrm{ds}}{D_\mathrm{s}}\,\boldsymbol{\delta}_\mathrm{O} = (1-x)\,\boldsymbol{\delta}_\mathrm{O}\,. \tag{77}$$

If one chooses x and y in the ecliptic plane and z towards the ecliptic north, where the sun is in the origin, positive x is into the direction of the perihelion and positive y is from the perihelion towards the earth's motion, the motion of the earth is given by

$$x(\xi(t)) \;=\; a_\oplus(\cos(\xi(t)) - \varepsilon)\,, \tag{78}$$

$$y(\xi(t)) \;=\; a_\oplus\sqrt{1-\varepsilon^2}\,\sin(\xi(t))\,, \tag{79}$$

where $\xi(t) \in [0, 2\pi)$ can be obtained from

$$2\pi\left(\frac{t-t_\mathrm{p}}{T} - \left\lfloor\frac{t-t_\mathrm{p}}{T}\right\rfloor\right) = \xi - \varepsilon\sin\xi\,. \tag{80}$$

This motion has to be projected to the lens plane which is towards the longitude φ and the latitude χ as defined before. Let the dimensionless coordinates in the lens plane be $\widetilde{x}_1, \widetilde{x}_2$, and let $\widetilde{x}_3$ be a coordinate perpendicular to the lens plane towards the observer, so that one gets a right-handed system. If one chooses $\widetilde{x}_1 = z$, $\widetilde{x}_2 = y$ and $\widetilde{x}_3 = -x$ for $\varphi = \chi = 0$, the angle φ gives a rotation around the $\widetilde{x}_1$-axis and the angle χ a following rotation around the $\widetilde{x}_2$-axis, so that one gets

$$\begin{pmatrix}\widetilde{x}_1\\ \widetilde{x}_2\end{pmatrix} = \frac{1-x}{r_\mathrm{E}}\,\mathscr{R}_2\begin{pmatrix}x(\xi(t))\\ y(\xi(t))\end{pmatrix} \tag{81}$$

with

$$\mathscr{R}_2 = \begin{pmatrix}-\sin\chi\cos\varphi & -\sin\chi\sin\varphi\\ -\sin\varphi & \cos\varphi\end{pmatrix} \tag{82}$$

and therefore, with

$$\rho' = \frac{a_\oplus(1-x)}{r_\mathrm{E}}\,, \tag{83}$$

one obtains

$$\widetilde{x}_1(t) \;=\; \rho'\Big[-\sin\chi\cos\varphi(\cos\xi(t)-\varepsilon) \;- \;-\sin\chi\sin\varphi\sqrt{1-\varepsilon^2}\,\sin\xi(t)\Big]\,, \tag{84}$$

$$\widetilde{x}_2(t) \;=\; \rho'\Big[-\sin\varphi(\cos\xi(t)-\varepsilon) \;+ \;+\cos\varphi\sqrt{1-\varepsilon^2}\,\sin\xi(t)\Big]\,. \tag{85}$$

The rotation around $\widetilde{x}_3$ by ψ finally gives

$$x_1(t) \;=\; \cos\psi\,\widetilde{x}_1(t) + \sin\psi\,\widetilde{x}_2(t)\,, \tag{86}$$

$$x_2(t) \;=\; -\sin\psi\,\widetilde{x}_1(t) + \cos\psi\,\widetilde{x}_2(t)\,. \tag{87}$$

Let p be the parameter along the source trajectory and d the distance perpendicular to it measured from a line parallel to the source trajectory through the origin. By choosing $v_\perp$ along x_1, I obtain

$$p(t) \;=\; \widetilde{p_0}(t) + \cos\psi\,\widetilde{x}_1(t) + \sin\psi\,\widetilde{x}_2(t)\,, \tag{88}$$

$$d(t) \;=\; \widetilde{d_0} - \sin\psi\,\widetilde{x}_1(t) \;+\cos\psi\,\widetilde{x}_2(t)\,, \tag{89}$$

where

$$\widetilde{p_0}(t) = \frac{t-\widetilde{t_\mathrm{max}}}{t_\mathrm{E}}\,. \tag{90}$$

One sees that for $t = \widetilde{t_\mathrm{max}}$, in general, $p(t) \neq 0$ and $d(t) \neq \widetilde{d_0}$. To avoid a change in the fit parameters when including the parallax (i.e. changing between heliocentric and geocentric coordinates), it is favourable to use the same fit parameters t_max and d_0 (which has been called u_min before) in both cases by subtracting the earth-sun distance at t_max, which yields for the coordinates $p(t)$ towards the direction of the source and $d(t)$ perpendicular to it

$$p(t) \;=\; p_0(t) + \cos\psi\,\big(\widetilde{x}_1(t) - \widetilde{x}_2(t_\mathrm{max})\big) \;+ \;+\sin\psi\,\big(\widetilde{x}_2(t) - \widetilde{x}_2(t_\mathrm{max})\big)\,, \tag{91}$$

$$d(t) \;=\; d_0 - \sin\psi\,\big(\widetilde{x}_1(t) - \widetilde{x}_1(t_\mathrm{max})\big) \;+ \;+\cos\psi\,\big(\widetilde{x}_2(t) - \widetilde{x}_2(t_\mathrm{max})\big)\,, \tag{92}$$

where

$$p_0(t) = \frac{t-t_\mathrm{max}}{t_\mathrm{E}}\,, \tag{93}$$

and the impact parameter is given by

$$u(t) = \sqrt{[d(t)]^2 + [p(t)]^2}\,. \tag{94}$$

The longitude φ and the latitude χ are related to the ecliptic coordinates β and λ in the following way. The ecliptic coordinates are geocentric but above a heliocentric system has been used. Therefore, the sun-around-earth motion has to be converted to an earth-around-sun motion. It can be seen that the vector $\boldsymbol{x}$ of the sun's position measured from the earth is transformed into a vector $-\boldsymbol{x}$ of the earth's position measured from the sun. Since the angular momentum $\boldsymbol{L}$ is an axial vector (which

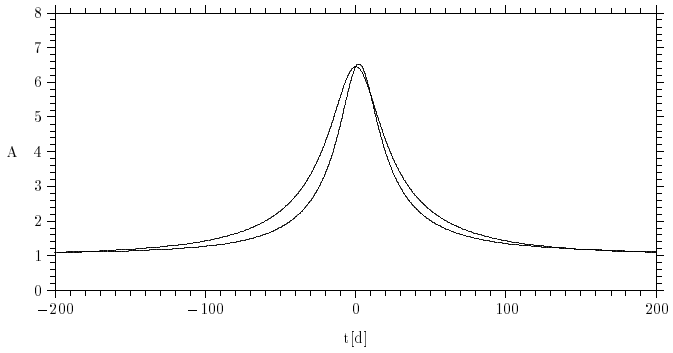

Fig. 5. Light curves with and without considering the earth's motion around the sun, the symmetric curve neglects the earth's motion

means that it does not change its sign under this transformation), the earth moves around the sun in the *same* direction as the sun moves around the earth in a geocentric system. Therefore, one sees that $\chi = \beta$, where the parallax is neglected, which does not play a role in determining the position, because we deal with distances of the order of 10 kpc. The ecliptical length is measured from the vernal equinox along the ecliptic in the same sense as the right ascension. Since the sun moves towards positive right ascension, λ increases with time t. The earth's motion around the sun is also in the direction of positive λ, so that $\varphi = \lambda + \varphi_c$ with a constant φ_c, if one neglects the earth-sun distance. The sun's position as seen from the earth corresponds to $\lambda = 0$ at vernal equinox, while the earth's position as seen from the sun corresponds to $\lambda = \pi$. If φ_γ denotes the longitude of the vernal equinox as measured from the perihelion, one obtains $\varphi_c = \pi + \varphi_\gamma$ and therefore $\varphi = \lambda + \pi + \varphi_\gamma$.

Inserting the definition of the Einstein radius, Eq. (36), into the definition of ρ', Eq. (83), yields

$$\rho' = \left(\frac{M}{M_\odot}\right)^{-1/2} \sqrt{\frac{a_\oplus^2}{2R_{S\odot}D_s}\,\frac{1-x}{x}} \tag{95}$$

for $x \neq 1$. One sees that ρ' diverges for $x \to 0$ and $\rho' \propto 1/\sqrt{M}$. For $x = \frac{1}{2}$, $D_s = 8$ kpc and $M = 1M_\odot$, $\rho' = 0.7$, while for $M = 10^{-5}\,M_\odot$, $\rho' = 23$.

In Fig. 5, a light curve where the earth's motion around the sun has been considered together with a light curve where this motion has been neglected is shown. Since both models use the same parameters, the amplification for $t = t_{max} = 0$ is the same. For this example, parameters which are similar to those of the parallax event found by the MACHO collaboration (Alcock et al. 1995) have been chosen. The eccentricity of the earth's orbit is $\varepsilon = 0.0167$, while its rotation period is $T = 365.26$ d. With the ecliptical coordinates $\lambda = 271°$ and $\beta = -5°$, and $\varphi_\gamma = 77°$ being the longitude of the vernal equinox measured from the perihelion, one obtains $\varphi = 2.93$ rad and $\chi = -0.08$ rad. Moreover, I have chosen $\psi = 4.14$ rad, $\rho' = 0.2$, $d_0 = -0.16$, $t_E = 110$ d, and $t_{max} = t_p = 0$.

8. Additional constraints on the mass and other physical quantities

For a microlensing event, the Einstein radius r_E, the lens mass M, the lens distance D_d and the transverse velocity $v_\perp$ cannot be observed directly in general. Any model for the lens and the source involves the timescale t_E, which gives the relation

$$r_E = t_E\, v_\perp\,, \tag{96}$$

so that r_E can be eliminated and 3 unknown quantities M, D_d and $v_\perp$, or alternatively $\mu = M/M_\odot$, $x = D_d/D_s$ and $v_\perp$ remain, which are related by the definition of the Einstein radius, which reads

$$t_E\, v_\perp = \sqrt{\frac{4GM_\odot}{c^2}\,D_s}\,\sqrt{\mu\, x(1-x)}\,. \tag{97}$$

Additional constraints may arise from certain models of the lens system. In the following, I discuss constraints from the finite source size, a rotating binary lens, and the parallax effect. Combining two of these allows to determine the lens distance (up to a possible degeneracy) and from this value the mass, the velocity, and the Einstein radius. Using three or more constraints will overdetermine the problem. However, one should note that there are uncertainties in the fit parameters.

8.1. Using one constraint

8.1.1. From extended sources

From the fit of an extended source, one obtains an additional constraint if the physical radius of the source r_s is known, which may be obtained approximately using the color and the absolute magnitude of the source. The parameter R_{src} is the ratio of the physical radius and the projected Einstein radius r'_E, i.e.

$$R_{src} = \frac{r_s}{r'_E} = \frac{x r_s}{r_E} = \frac{x r_s}{t_E\, v_\perp}\,, \tag{98}$$

which is an additional constraint between $v_\perp$ and x, i.e.

$$v_\perp(x) = \frac{x r_s}{t_E\, R_{src}}\,. \tag{99}$$

Since $x \in (0,1)$, one obtains a limit for $v_\perp$:

$$v_\perp < \frac{r_s}{t_E R_{src}}\,. \tag{100}$$

Using the constraint of Eq. (99), the lens mass can be written as a function of x

$$\mu(x) = \frac{c^2}{4GM_\odot D_s}\,\frac{r_s^2}{R_{src}^2}\,\frac{x}{1-x}\,, \tag{101}$$

or as a function of $v_\perp$

$$\mu(v_\perp) = \frac{c^2}{4GM_\odot D_s}\,\frac{t_E v_\perp r_s^2}{R_{src}(r_s - t_E v_\perp R_{src})}\,. \tag{102}$$

8.1.2. From the observer's motion around the sun

If one takes into account the observer's motion around the sun, one has the additional parameter ρ', which is related to the earth-sun distance $a_\oplus$ by

$$\rho' = \frac{a_\oplus(1-x)}{r_\mathrm{E}} = \frac{a_\oplus(1-x)}{t_\mathrm{E} v_\perp}\,, \tag{103}$$

giving a constraint between x and $v_\perp$, i.e.

$$v_\perp(x) = \frac{a_\oplus(1-x)}{t_\mathrm{E}\rho'}\,. \tag{104}$$

Since $x \in (0,1)$, one has

$$v_\perp < \frac{a_\oplus}{t_\mathrm{E}\rho'}\,. \tag{105}$$

The mass as a function of x follows as (compare Alcock et al. 1995)

$$\mu(x) = \frac{c^2}{4GM_\odot D_\mathrm{s}}\,\frac{a_\oplus^2}{\rho'^2}\,\frac{1-x}{x}\,, \tag{106}$$

and as a function of $v_\perp$ as

$$\mu(v_\perp) = \frac{c^2}{4GM_\odot D_\mathrm{s}}\,\frac{t_\mathrm{E} v_\perp a_\oplus^2}{\rho'(a_\oplus - t_\mathrm{E} v_\perp \rho')}\,. \tag{107}$$

8.1.3. From a rotating binary lens

For a rotating binary lens, one obtains from the orbital motion

$$T = 2\pi\sqrt{\frac{a^3}{GM}} = 2\pi t_\mathrm{E}^{3/2} v_\perp^{3/2}\sqrt{\frac{\rho^3}{GM_\odot\mu}}\,. \tag{108}$$

This yields the following pairwise relations:

$$\mu(v_\perp) = \frac{4\pi^2 t_\mathrm{E}^3\rho^3}{GM_\odot T^2}\,v_\perp^3\,, \tag{109}$$

$$\mu(x) = \frac{T^4c^6}{1024\pi^4 GM_\odot\rho^6}\,\frac{1}{D_\mathrm{s}^3\,x^3(1-x)^3}\,, \tag{110}$$

$$v_\perp(x) = \frac{T^2c^2}{16\pi^2 t_\mathrm{E}\rho^3}\,\frac{1}{D_\mathrm{s}\,x(1-x)}\,. \tag{111}$$

Since $x \in (0,1)$, $v_\perp$ is restricted to

$$v_\perp \geq \frac{T^2c^2}{4\pi^2 t_\mathrm{E}\rho^3 D_\mathrm{s}}\,. \tag{112}$$

8.2. Using two constraints

8.2.1. From an extended source and the observer's motion around the sun

Setting equal the expressions for the mass as a function of x for the extended source (Eq. (101)) and for the observer's motion around the sun (Eq. (106)), yields

$$\frac{x^2}{(1-x)^2} = \frac{a_\oplus^2 R_\mathrm{src}^2}{\rho'^2 r_\mathrm{s}^2}\,. \tag{113}$$

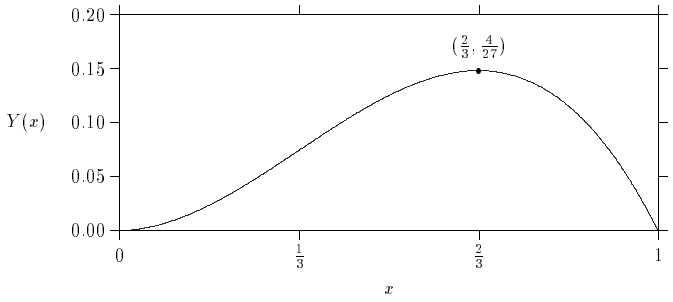

Fig. 6. $Y(x)$

Since one has

$$\frac{x}{1-x} > 0 \tag{114}$$

for $x \in (0,1)$, only the positive root is an appropriate solution, and one obtains

$$\frac{x}{1-x} = \frac{a_\oplus R_\mathrm{src}}{\rho' r_\mathrm{s}} \equiv X\,. \tag{115}$$

Solving for x yields the solution

$$x = \frac{X}{1+X} = \frac{a_\oplus R_\mathrm{src}}{\rho' r_\mathrm{s} + a_\oplus R_\mathrm{src}} \tag{116}$$

and from Eq. (99) or Eq. (104) one obtains for $v_\perp$

$$v_\perp = \frac{a_\oplus r_\mathrm{s}}{t_\mathrm{E}(\rho' r_\mathrm{s} + a_\oplus R_\mathrm{src})}\,. \tag{117}$$

8.2.2. From an extended source and a rotating binary lens

From the expressions for the mass as a function of x (Eq. (101) and Eq. (110)) one obtains the relation

$$(1-x)x^2 = \frac{T^2c^2 R_\mathrm{src}}{16\pi^2\rho^3 D_\mathrm{s} r_\mathrm{s}} \equiv Y\,. \tag{118}$$

Y as a function of x is shown in Fig. 6. Note that $x \in (0,1)$. The function has zeros for the boundary values $x = 0$ and $x = 1$ and a maximum at $(\frac{2}{3}, \frac{4}{27})$. Therefore, Y is restricted to $Y \in (0, \frac{4}{27}]$, which is a consequence from the constraint on the Einstein radius, which cannot exceed

$$r_\mathrm{E,max} = \sqrt{\frac{GMD_\mathrm{s}}{c^2}}\,. \tag{119}$$

For any value of Y, there are two values of x, except for $Y = Y_\mathrm{max} = \frac{4}{27}$. For given x, the mass M, the Einstein radius r_E and the absolute value of the transverse velocity can be successively calculated.

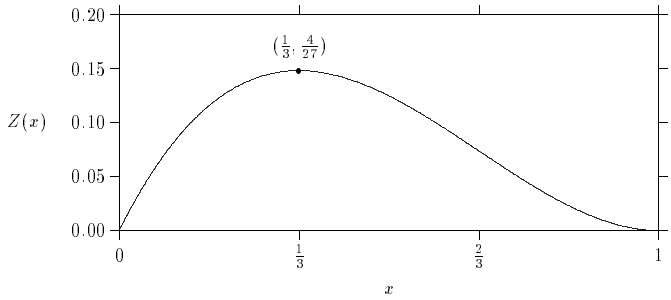

Fig. 7. $Z(x)$

8.2.3. From the observer's motion around the sun and a rotating binary lens

From Eq. (106) and Eq. (110) one obtains

$$x(1-x)^2 = \frac{T^2c^2}{16\pi^2 D_{\rm s} a_\oplus}\,\frac{\rho'}{\rho^3} \equiv Z\,. \tag{120}$$

Z as a function of x is shown in Fig. 7. Note that $Z(x) = Y(1-x)$. . The function has zeros for $x = 0$ and $x = 1$ and a maximum at $(\frac{1}{3}, \frac{4}{27})$. Since $x \in (0,1)$, Z is restricted to $Z \in (0, \frac{4}{27}]$. For any value of Z, there are two values of x, except for $Z = Z_{\rm max} = \frac{4}{27}$.

8.3. Using three constraints

With all three constraints, x should be a similar solution to $X(x)$, $Y(x)$, and $Z(x)$. Since $X(x)$ yields a unique solution, one of the solutions of $Y(x)$ and $Z(x)$ has to be dropped. Note that

$$X = \frac{Y}{Z}\,. \tag{121}$$

Since the fit parameters and the source radius $r_{\rm s}$ contain uncertainties, one may fit for a most-likely value of x.

9. A fit with a rotating binary lens for DUO#2

The DUO#2 event has been reported by Alard et. al (1995), where a fit with a strong binary lens is presented. I have investigated some more possible fits using a static binary lens and a point source (Dominik 1997b). Here I show the results of a fit with a rotating binary lens with parameters which are completely different from the fits with static binaries. I have omitted one occurence of a data point which appeared twice in the data I have received from C. Alard, so that I use 115 data points and not 116 data points as in (Alard et al. 1995). Moreover, I use the magnitude values for the fit and not the amplification values. The parameters for the fit are shown in Table 4, while the resulting light curves are shown in Fig. 8. The $\chi^2_{\rm min}$ indicates that this fit can be marginally accepted.

Note that the peak after the second caustic crossing is to some part due to the rotation and that R_T is 0.07.

If one adopts a transverse velocity of $v_\perp = 30$ km/s, one obtains, using Eq. (109), a total mass of the lens of $M = 0.025\ M_\odot$, i.e. one object with $M_1 = 5.9{\cdot}10^{-3}\ M_\odot$ and one object with mass $M_2 = 0.019\ M_\odot$. The Einstein radius becomes $r_{\rm E} = 0.11$ AU and the semimajor axis $a = 0.12$ AU. However, the lens distance parameter x follows as 0.993 or 0.007, which seems improbable. Taking 0.993, i.e. the lens close to the source, as the more probable configuration, one can understand the lens more easily if it is in the bulge population rather than in the disk population. However, this value is very extreme, a value of 0.9 or 0.95 would have been more plausible, but there is some room in the uncertainty of the velocity[5] and of the fit parameters. Anyway, I have tried this model mainly to show that there are parameters for a rotating binary model distinct from the static ones which produce the light curve, without assuming that a physically reasonable model would result.

As noted in Sect. 5, long timescales $t_{\rm E}$ are favoured for showing rotation effects and the timescale for DUO#2 is rather short. It is interesting to see how the situation changes if an event would have been observed whose light curve shows the same shape as that of DUO#2 but whose timescale is 10 times larger. For this hypothetical event, the only changes in the fit parameters compared to DUO#2 would be an enlargement in $t_{\rm E}$ and T by a factor of 10. For the same transverse velocity $v_\perp = 30$ km/s, the Einstein radius $r_{\rm E}$ would be 10 times larger and, according to Eqs. (109) and (111), the mass M and $x(1-x)$ would increase by the same factor, yielding $M_1 = 0.059\ M_\odot$,

[5] Note that $M \sim v_\perp^3$.

Table 4. Fit for DUO#2 using a model with a rotating binary lens

parameter	value
$t_{\rm E}$ [d]	6.4
t_b [d]	85.40
ρ	1.058
m_1	0.238
α [rad]	2.374
b	-0.087
$m_{\rm base,blue}$	-20.198
$m_{\rm base,red}$	-18.564
$f_{\rm blue}$	0.563
$f_{\rm red}$	0.547
β [rad]	0.958
γ [rad]	0.358
T [d]	92.4
ε	0
ξ_0	-0.046
$\chi^2_{\rm min}$	120.51
n = # d.o.f.	100
$\sqrt{2\chi^2_{\rm min}} - \sqrt{2n-1}$	1.418
$P(\chi^2 \geq \chi^2_{\rm min})$	8 %

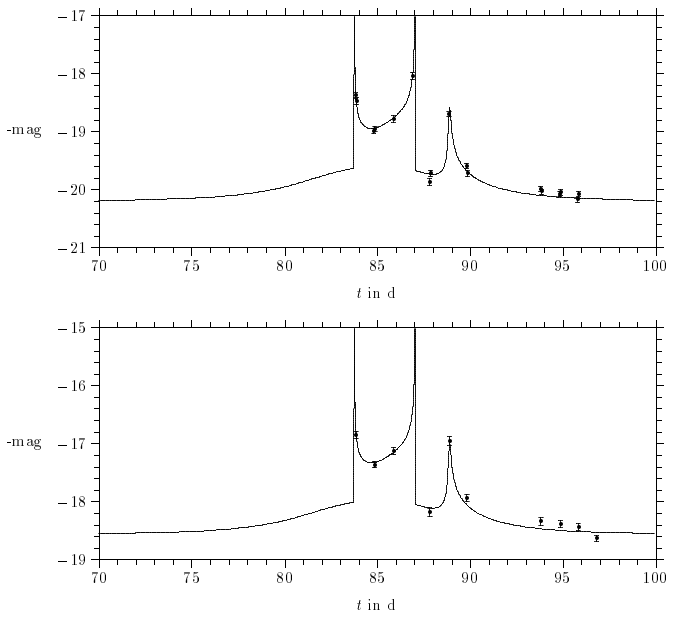

Fig. 8. DUO #2: Light curve for a rotating binary lens together with the data. Light curve for the blue spectral band on the top and light curve for the red spectral band on the bottom.

$M_2 = 0.19\ M_\odot$, $r_\mathrm{E} = 1.1$ AU, $a = 1.2$ AU, and $x = 0.92$, i.e. more reasonable values, so that the light curve (whose shape is identical to that of DUO#2) may well be explained by this rotation effect. This shows that it is worth trying fits with rotating binary lenses.

10. Summary

Rotating binaries are a reality both in the universe and among galactic microlensing observations. They are helpful in providing additional information about physical parameters of the lens system and they may also be used to assign probabilities to fits using the knowledge on the distribution of their parameters. The inclusion of the rotation for binary lenses enlarges the parameter space and gives room for additional parameter degeneracies. It also provides additional shapes of light curves through the motion of the caustics. Every fit with a static binary should be checked for consistency.

Acknowledgements. I would like to thank S. Mao for some discussions on the subject and for useful comments, C. Alard for sending me the data of the DUO#2 event, the OGLE collaboration for making available their data, and the MACHO collaboration for making available the MACHO LMC#1 data.

Appendix A: approximation of the trajectory to first order in ε

Here I show that the expressions for parallax light curves given by Alcock et. al (1995) are reproduced by expanding the trajectory to first order in the eccentricity ε. One obtains the earth's trajectory in the form (e.g. Montenbruck & Pfleger 1989)

$$\begin{pmatrix} x(t) \\ y(t) \end{pmatrix} = A(t) \begin{pmatrix} \cos\xi(t) \\ \sin\xi(t) \end{pmatrix} \tag{A1}$$

with

$$A(t) = a_\oplus \left(1 - \varepsilon \cos\left(2\pi \frac{t-t_\mathrm{p}}{T}\right)\right) \tag{A2}$$

$$\xi(t) = 2\pi \frac{t-t_\mathrm{p}}{T} + 2\varepsilon \sin\left(2\pi \frac{t-t_\mathrm{p}}{T}\right) . \tag{A3}$$

With

$$A'(t) = A(t)\frac{1-x}{r_\mathrm{E}} \tag{A4}$$

the lens plane coordinates $\widetilde{x}_1(t)$ and $\widetilde{x}_2(t)$ follow from Eq. (81) as

$$\begin{aligned} \widetilde{x}_1(t) &= A'(t)\,[-\sin\chi\cos\varphi\cos\xi(t) - \\ &\quad - \sin\chi\sin\varphi\sin\xi(t)]\ , \end{aligned} \tag{A5}$$

$$\widetilde{x}_2(t) = A'(t)\,[-\sin\varphi\cos\xi(t) + \cos\varphi\sin\xi(t)]\ . \tag{A6}$$

For $\varphi = 0$ one has

$$\widetilde{x}_1(t) = -A'(t)\sin\chi\cos\xi(t)\,, \tag{A7}$$

$$\widetilde{x}_2(t) = A'(t)\sin\xi(t)\,, \tag{A8}$$

and therefore

$$\begin{aligned} d(t) &= \widetilde{d}_0 + A'(t)\cos\psi\sin\xi(t) + \\ &\quad + A'(t)\sin\psi\sin\chi\cos\xi(t)\,, \end{aligned} \tag{A9}$$

$$\begin{aligned} p(t) &= \widetilde{p_0}(t) - A'(t)\cos\psi\sin\chi\cos\xi(t) + \\ &\quad + A'(t)\sin\psi\sin\xi(t)\,. \end{aligned} \tag{A10}$$

For the distance from the origin $u(t)$ one gets

$$\begin{aligned} u^2(t) &= [d(t)]^2 + [p(t)]^2 = \widetilde{d_0}^{\,2} + \widetilde{p_0}^{\,2} + A'^2\sin^2\xi + \\ &\quad + A'^2\sin^2\chi\cos^2\xi + \\ &\quad + 2A'\sin\xi[\widetilde{d_0}\cos\psi + \widetilde{p_0}\sin\psi] + \\ &\quad + 2A'\sin\chi\cos\xi[\widetilde{d_0}\sin\psi - \widetilde{p_0}\cos\psi]\,. \end{aligned} \tag{A11}$$

The rotation in the ecliptic plane by an angle φ is equivalent to a shift in $\xi(t)$. This means that one has

$$\xi(t) = 2\pi \frac{t-t_\mathrm{p}}{T} + 2\varepsilon \sin\left(2\pi \frac{t-t_\mathrm{p}}{T}\right) - \varphi = \xi_0(t) - \varphi\,. \tag{A12}$$

Inserting $\xi(t)$ into Eqs. (A7) and (A8) reveals the expressions given in Eqs. (A5) and (A6) where $\xi(t)$ has to be replaced by $\xi_0(t)$.

The MACHO collaboration (Alcock et al. 1995) find that

$$\begin{aligned} u^2(t) &= u_0^2 + \omega^2(t-t_0)^2 + \alpha^2\sin^2[\Omega(t-t_\mathrm{c})] \\ &\quad + 2\alpha\sin[\Omega(t-t_\mathrm{c})][\omega(t-t_0)\sin\theta + u_0\cos\theta] + \\ &\quad + \alpha^2\sin^2\beta\cos^2[\Omega(t-t_\mathrm{c})] + \\ &\quad + 2\alpha\sin\beta\cos[\Omega(t-t_\mathrm{c})]\ \cdot \\ &\quad \cdot [\omega(t-t_0)\cos\theta - u_0\sin\theta]\,, \end{aligned} \tag{A13}$$

where

$$\alpha = \frac{\omega a_\oplus}{\tilde{v}} \left(1 - \varepsilon \cos[\Omega_0(t - t_\mathrm{p})]\right) \tag{A14}$$

and

$$\Omega(t - t_\mathrm{c}) = \Omega_0(t - t_\mathrm{c}) + 2\varepsilon \sin[\Omega_0(t - t_\mathrm{p})]\,, \tag{A15}$$

where $\Omega_0 = 2\pi/T$ and $\tilde{v} = v_\perp/(1 - x)$.

This expression is equivalent to the derived one with $\alpha = A'$, $u_0 = \widetilde{d}_0$, $\Omega(t-t_\mathrm{c}) = \xi$, $\widetilde{p}_0 = -\omega(t-t_0)$, $\theta = -\psi$, $\varphi = \Omega_0(t_\mathrm{c}-t_\mathrm{p})$. Note the sign in $\widetilde{p}_0$ and θ, which is due to the fact that I define the lens to be on the right side of the moving source, while the MACHO collaboration lets the source move in the opposite direction. Further note that their replacement of φ by $\Omega_0(t_\mathrm{c}-t_\mathrm{p})$ is an approximation and that t_c is the point of time where the earth is closest to the sun-source line. Finally note that $\omega = 1/t_\mathrm{E}$ and

$$\rho' = \frac{\omega a_\oplus}{\widetilde{v}} = \frac{a_\oplus}{t_\mathrm{E}\widetilde{v}}\,. \tag{A16}$$

References

Alard C., Mao S., Guibert J., 1995, A&A 300, L17
Alcock C., Allsman R. A., Alves D., et al., 1995, ApJ 454, L125
Ansari R., Cavalier F., Couchot F., et al., 1995, A&A 299, 168
Dominik M., 1997a, Estimating physical quantities for an observed galactic microlensing event, preprint astro-ph/9701035, submitted (D97a)
Dominik M., 1997b, Ambiguities in fits of observed galactic microlensing events, preprint astro-ph/9702039, submitted
Dominik M., Hirshfeld A. C., 1996, A&A 313, 841
Gould A., 1992, ApJ 392, 442
Griest K., Hu W., 1992, ApJ, 397, 362 (Erratum: 1993, ApJ 407, 440)
Landau L. D., Lifshitz E. M., 1969, Mechanics, Volume 1 of Course of Theoretical Physics, 2nd edition, Pergamon Press, Oxford
Montenbruck O., Pfleger T., 1989, Astronomie mit dem Personal Computer, Springer, Berlin
Paczyński B., 1986, ApJ 304, 1
Paczyński B., 1996, ARA&A 34, 419
Schneider P., Ehlers J., Falco E. E., 1992, Gravitational Lenses, Springer, Berlin

This article was processed by the author using Springer-Verlag LaTeX A&A style file *L-AA* version 3.